TECHNICAL REPORT ARLCD-TR-83048

# THEORETICAL CALCULATIONS OF H(2) CARS SPECTRA FOR PROPELLANT FLAMES

JOANNE FENDELL
L. E. HARRIS
KENNETH ARON

DECEMBER 1983


U.S. ARMY ARMAMENT RESEARCH AND DEVELOPMENT CENTER
LARGE CALIBER WEAPON SYSTEMS LABORATORY
DOVER, NEW JERSEY

# REPORT DOCUMENTATION PAGE

READ INSTRUCTIONS BEFORE COMPLETING FORM

1. REPORT NUMBER: Technical Report ARLCD-TR-83048
2. GOVT ACCESSION NO.:
3. RECIPIENT'S CATALOG NUMBER:

4. TITLE (and Subtitle): THEORETICAL CALCULATIONS OF H(2) CARS SPECTRA FOR PROPELLANT FLAMES

5. TYPE OF REPORT & PERIOD COVERED:

6. PERFORMING ORG. REPORT NUMBER:

7. AUTHOR(s):
Joanne Fendell
L. E. Harris
Kenneth Aron

8. CONTRACT OR GRANT NUMBER(s):

9. PERFORMING ORGANIZATION NAME AND ADDRESS
ARDC, LCWSL
Applied Sciences Div [DRSMC-LCA-G(D)]
Dover, NJ 07801

10. PROGRAM ELEMENT, PROJECT, TASK AREA & WORK UNIT NUMBERS:
1L16122AH60

11. CONTROLLING OFFICE NAME AND ADDRESS
ARDC, TSD
STINFO Div [DRSMC-TSS(D)]
Dover, NJ 07801

12. REPORT DATE: December 1983

13. NUMBER OF PAGES: 29

14. MONITORING AGENCY NAME & ADDRESS (if different from Controlling Office):

15. SECURITY CLASS. (of this report): Unclassified

15a. DECLASSIFICATION/DOWNGRADING SCHEDULE:

16. DISTRIBUTION STATEMENT (of this Report)
Approved for public release; distribution unlimited.

17. DISTRIBUTION STATEMENT (of the abstract entered in Block 20, if different from Report)

18. SUPPLEMENTARY NOTES

19. KEY WORDS (Continue on reverse side if necessary and identify by block number)
CARS
Propellant
Hydrogen
Rotational raman
Vibrational raman

20. ABSTRACT (Continue on reverse side if necessary and identify by block number)
High energy pure rotational H(2) CARS transitions have recently been observed in several spectral regions, most notably, the NO and CO CARS regions. H(2) CARS is of interest because hydrogen is a major combustion product of propellants, especially nitramine propellants. For this reason, calculations were performed to assign the observed H(2) transitions.

(cont)

20. ABSTRACT (cont)

For this particular case, the calculations of interest are for the observed S- and Q-branch transitions of H(2) for v equal to 0 and 1. Spectroscopic constants available in the literature and the results of an ab initio calculation performed by Ermler were used in the analysis.

Ermler used the potential energy curves for the ground state of hydrogen calculated by Kolos and Wolniewicz over a range of $0.4 \leq R \leq 10.0$ a.u. as the basis for this calculation. The result is a set of spectroscopic constants superior to any other set examined.

Having assigned the transitions, the third order susceptibility, which gives a model for data reduction of CARS spectra can be calculated. Temperature and concentration for a given species can be obtained by comparing the theoretical spectra with experimental results.

ACKNOWLEDGMENT

The authors would like to thank Professor W. C. Ermler, Stevens Institute of Technology, for providing us with the *ab initio* calculations and helpful discussions.

CONTENTS


| | Page |
|---|---|
| Introduction | 1 |
| CARS Theory | 1 |
| Results | 2 |
| Spectroscopic Constants | 2 |
| Application of Spectroscopic Constants | 2 |
| Calculation of $H_2$ CARS S- and Q-Branches | 3 |
| Discussion | 4 |
| References | 5 |
| Distribution List | 15 |


TABLES


| | | Page |
|---|---|---|
| 1 | Comparison of spectroscopic constants ($cm^{-1}$) | 7 |
| 2 | Calculation of selected transitions ($cm^{-1}$) | 7 |
| 3 | Computed energies of $H_2$ Q-branch transitions | 8 |
| 4 | Computed energies of $H_2$ S-branch transitions | 9 |


FIGURES


| | | |
|---|---|---|
| 1 | $H_2$ CARS Q-branch spectra at 2500 K | 11 |
| 2 | $H_2$ CARS Q-branch spectra at 3000 K | 11 |
| 3 | Temperature variation of $H_2$ CARS spectra | 12 |
| 4 | $H_2$ CARS S-branch at 2732 K | 13 |

## INTRODUCTION

The use of coherent anti-stokes Raman scattering (CARS) spectroscopy in combustion studies is well documented (refs 1 through 5). Hydrogen is a major combustion product of propellants, as illustrated by $H_2$ CARS S-branch transitions, obtained from both $CH_4/N_2O$ model propellant flames and actual propellant flames (refs 6 and 7).

Because the use of $H_2$ CARS spectra to obtain temperature and concentration profiles is limited by the reliability of the spectroscopic constants, a literature search was conducted (refs 8 through 11) to find a suitable set of spectroscopic constants, and a set of ab initio calculations were obtained from Ermler.[1] The method used by Ermler is described briefly below. A more complete treatment is given in the literature (refs 12 through 15). Overall the transition energies calculated on the basis of Ermler's constants agreed most closely with our experimental results, so that particular set of spectroscopic constants was used to calculate $H_2$ S- and Q-branches.

## CARS THEORY

The observed CARS spectrum is proportional to the square of the modulus of the third order susceptibility, $\chi^{(3)}$, which is the sum of a resonant term $\chi_r$, and a nonresonant term $\chi_{nr}$, which are related to the vibrational and electronic displacement, respectively

$$\chi^{(3)} = \chi_r + \chi_{nr} \tag{1}$$

The resonant term is calculated as the sum of Lorentian line shapes of each rotational transition

$$\chi_r = \sum_j K_j \Gamma_j / (2\Delta\omega_j - i\Gamma_j) \tag{2}$$

given that

$$K_j = \frac{2N}{h} |\alpha_j|^2 (\Delta p_j^{(0)}) \Gamma_j^{-1} \tag{3}$$

where N is the number density, $\alpha_j$ is the isotropic polarizability matrix element for the transition, $\Delta p_j^{(0)}$ is the normalized population difference between the

---

[1] Personal communication between W. C. Ermler, Stevens Institute of Technology, Hoboken, NJ and J. Fendell, ARDC, May 1983.

molecular energy levels involved in the transition, $\omega_j$ is the isolated pressure-broadened linewidth, and $\Delta\omega_j = \omega_1 - \omega_2 - \omega_j$. The calculated $|\chi^{(3)}|^2$ is first convoluted over the laser shapes, then over a triangular slit function.

$\chi_r$ is the sum of real and imaginary components $\chi'$ and $\chi''$, respectively, so that

$$|\chi^{(3)}|^2 = \chi'^2 + 2\chi'\chi_{nr} + \chi''^2 + \chi_{nr}^2 \qquad (4)$$

$\chi'$ and $\chi''$ display dispersive and resonant behavior with respect to the detuning frequency, $\Delta\omega_j$.

As the concentration of the resonant species is lowered, the cross term $2\chi'\chi_{nr}$, which is dispersive, influences the shape of the spectrum. The observation of dispersively modulated spectra allows temperature and concentration to be estimated on the basis of model calculations.

The concentration of various species from the ratio of the total CARS intensity to the nonresonant intensity at any frequency where resonant transition of the species occurs can also be estimated. In broadband CARS, the nonresonant susceptibility is usually observed directly from regions where no resonance occurs. The spectral distribution of the nonresonant susceptibility, which reflects that of $\omega_2$, can be obtained either from measurements of the distribution of $\omega_2$ or directly from measurements of a nonresonant gas (ref 16).

## RESULTS

### Spectroscopic Constants

In an effort to find theoretical support for experimental observations, a literature search for spectroscopic constants for the $X\,^1\Sigma_g^+$ state of hydrogen was conducted. Constants published by Stoicheff (ref 8), Fink et al. (ref 9), Herzberg (ref 10), and Huber and Herzberg (ref 11) were available in the literature. Another set was obtained by data reduction of the results obtained from Ermler.

In his calculations, Ermler used potential energy curves for the $X\,^1\Sigma_g^+$ state of hydrogen calculated by Kolos and Wolniewicz (ref 13). These potential curves are obtained by using a generalized James-Coolidge wavefunction with variational parameters in elliptic coordinates, which is then used to solve the Schrodinger equation by numerical methods. Double precision arithmetic using 15 vibrational and 15 rotational levels were used in the calculations.

### Application of Spectroscopic Constants

The total energy of a molecule is a function of both the rotational and vibrational quantum numbers. The expression is given as

$$E(v,J) = \omega_e(v + 0.5) - X_e\omega_e(v + 0.5)^2 + Y_e\omega_e(v + 0.5)^3 - Z_e\omega_e(v + 0.5)^4 +$$

$$B_v(J^2 + J) - D_v J^2(J + 1)^2 + H_v(J^3)(J + 1)^3$$

where

$$B_v = Be + \alpha_e(v + 0.5) + \gamma_e(v + 0.5)^2$$

$$D_v = De + \beta(v + 0.5) + \delta_e(v + 0.5)^2$$

$$H_v = H_0 + H_1(v + 0.5) + H_2(v + 0.5)^2$$

It is useful to know the values of $B_v$, $D_v$, and $H_v$, since they allow us to predict the frequencies at which pure rotational (S-branch) and ro-vibrational (Q-branch) transitions will occur.

S-branch = E(I,J+2)-E(I,J)

Q-branch = E(I+1,J)-E(I,J)

In general, $B_v$, $D_v$, and $H_v$ are approximated by second-order polynomials. Stoicheff, Herzberg, and Huber and Herzberg stated these polynomials explicitly, but Fink et al. and Ermler stated these quantities at various values of v. In order to use these values in a systematic way in calculating S-branch and Q-branch specta, values of $B_v$, $D_v$, and $H_v$ corresponding to v = 0,1,2 were fitted to a second-order polynomial. The estimated standard error for these correlations ranged between $10^{-3}$ and $10^{-18}$ for Fink's results and between $10^{-11}$ and $10^{-18}$ for Ermler's results. The values for $B_v$, $D_v$, and $H_v$ from all sources are compiled in table 1.

In table 2, the calculated S-branch frequencies are compared to our recently obtained experimental results. There is a clear difference among the results obtained by using various constants to calculate higher S-branch transitions. The constants of Fink et al. and Ermler were used to calculate the transition frequencies found in tables 3 and 4, since these particular sets of constants agreed most closely with experimental results.

## Calculation of $H_2$ CARS S- and Q-Branches

$H_2$ CARS S- and Q-branches were calculated using Ermler's spectroscopic constants. The Q-branch results for various temperatures are given in figures 1, 2, and 3. The S-branch results shown in figure 4 for the $S_o(7,5)$[2], transition at 1815 $cm^{-1}$ illustrates conditions comparable to those in the $\phi = 1.8$ $CH_4/N_2O$ flame

---

[2] S-branch transitions are labeled using the notation $S_v(J', J'')$.

in which it was observed (refs 6 and 7). In these calculations, a Doppler broadened linewidth and a 3.0 $cm^{-1}$ slit function were assumed.

## DISCUSSION

The recently observed higher S-branch transitions (refs 6 and 7) are compared to the transition frequencies given by various spectroscopic constants in table 2. In all cases, the constants of Fink et al. and Ermler agree more closely with experimental results than other constants. For the v = 0 transitions, the results of Fink et al. and Ermler diverge as the transitions increase in frequency. Ermler's results are closer to the experimental results for $S_o(9,7)$ than those of Fink et al. For $S_o(11,9)$, the difference between experimental results and those of Fink et al. is large enough to be experimentally discernible. The frequency of the $S_o(11,9)$ transition has been observed experimentally at 2131 $cm^{-1}$ by us (refs 6 and 7) as well as Farrow et al. (ref 17) in good agreement with Ermler's value of 2130 $cm^{-1}$. The results obtained for v = 1 do not differ greatly for either set of constants until levels higher than the observed transitions are reached. On the basis of present experimental data, Ermler's constants agree most closely with the experiment.

For both v = 0 and v = 1, Ermler's constants predict that the Q-branch transitions will be more closely spaced than the results of Fink et al. As seen from the computed results (table 3), Ermler's constants predict experimentally discernable differences from those at Fink et al. (ref 18) beginning at J''=6. The computed CARS Q-branch spectra (fig. 1 and 1a) show that above 2500 K, Q-branches above J''=6 are significantly populated. Q-branch spectra will be taken to confirm the validity of the spectroscopic constants at these temperatures.

The results obtained indicate that the set of spectroscopic constants obtained from the ab initio calculations are in better agreement with experimental results than other sets of constants.

REFERENCES


1. R. L. Farrow, P. L. Mattern, and L. A. Rahn, Applied Optics, vol 21, 1982, p 3119.

2. R. J. Hall and A. C. Eckbreth, Optical Engineer, vol 20, 1981, p 494.

3. S. Druet and J. P. Taran, Chemical and Biological Applications of Lasers, C. B. Moore, ed, Academic Press, New York, NY, 1979.

4. J. W. Nibler and G. V. Knighten, Raman Spectroscopy of Gases and Liquids, A. Weber, ed, Springer-Verlag, New York, NY, 1979.

5. L. E. Harris, "CARS Spectroscopy of Propellant Flames," Proceedings of the 9th International Colloquium on Dynamics of Explosives and Reactives Systems, Poitier, France, 1983.

6. L. E. Harris, K. Aron, J. Fendell, 19th JANNAF Combustion Meeting, Greenbelt, MD, 1982.

7. K. Aron, L. E. Harris, J. Fendell, Applied Optics, to be published.

8. B. P. Stoicheff, Raman Spectroscopy of Gases, vol IX, 1957.

9. U. Fink et al., J. Mol Spect, vol 18, 1965, p 384.

10. G. Herzberg, Spectra of Diatomic Molecules, Van Nostrand, New York, NY, 1950.

11. K. P. Huber and G. Herzberg, Constants of Diatomic Molecules, Van Nostrand, New York, NY, 1979.

12. W. Kolos and L. Wolniewicz, J. of Chemical Physics, vol 43, 1965, p 2429.

13. J. W. Cooley, Math Computations, vol 15, 1961, p 363.

14. W. Kolos and L. Wolniewicz, J. of Chemical Physics, vol 49, 1968, p 404.

15. W. Kolos and L. Wolniewicz, J. of Chemical Physics, vol 41, 1974, p 3663.

16. L. E. Harris, Combustion and Flame, vol 53, pp 103-121, 1983.
L. E. Harris, Chemical Physics Letters, vol 93, 1982, p 335.

17. R. Farrow, P. Mattern, and L. A. Rahn, 7th International Raman Conference, Ottawa, Ontario, Canada, 1980, p 668.

18. K. Aron and L. E. Harris, 20th JANNAF Combustion Meeting, Monterey, CA, 1983.

Table 1. Comparison of spectroscopic constants ($cm^{-1}$)

| Constants | Herzberg | Huber and Herzberg | Stoicheff | Fink et al. | Ermler |
|---|---|---|---|---|---|
| Be | 60.800 | 60.853 | 60.840 | 60.8318 | 60.7922 |
| $\alpha_e$ | -2.993 | -3.062 | -3.0177 | -3.0087 | -3.0320 |
| $\beta_e$ | 0.025 | 0.057 | 0.0285 | 0.0266 | 0.0350 |
| De | 0.0464 | 0.00471 | 0.04684 | 0.0471 | 0.0448 |
| Be | -0.00134 | -0.0027 | -0.0017 | -0.0029 | -0.0016 |
| $\delta e$ | -- | 0.0004 | $3 \times 10^{-5}$ | $4.5 \times 10^{-4}$ | $4.5 \times 10^{-5}$ |
| $H_o$ | $5.18 \times 10^{-5}$ | -- | $5.2 \times 10^{-5}$ | $5.62 \times 10^{-6}$ | $3.23 \times 10^{-5}$ |
| $H_1$ | -- | -- | -- | $-1.7 \times 10^{-6}$ | $-8.70 \times 10^{-7}$ |
| $H_2$ | -- | -- | -- | $4 \times 10^{-7}$ | $-2.50 \times 10^{-8}$ |
| $\omega e$ | 4395.2 | 4401.21 | 4401.21 | 4401.217 | 4400.39 |
| $\chi e \omega e$ | 117.90 | 121.33 | 121.43 | 121.343 | 120.814 |
| $ye\omega e$ | 0.29 | 0.812 | 0.892 | 0.8145 | 0.7241 |
| $Ze\omega e$ | 0. | 0. | 0. | 0. | 0. |

Table 2. Calculation of selected transitions ($cm^{-1}$)

| Transition[a] | Experimental[b] | Stoicheff | Fink et al. | Ermler | Huber and Herzberg |
|---|---|---|---|---|---|
| $S_o(7,5)$ | 1446 | 1447.67 | 1447.61 | 1447.80 | 1449.83 |
| $S_o(9,7)$ | 1809 | 1817.95 | 1817.18 | 1815.08 | 1822.05 |
| $S_o(11,9)$ | 2131 | 2145.01 | 2141.91 | 2130.32 | 2150.30 |
| $S_1(9,7)$ | 1721 | 1725.42 | 1719.90 | 1721.81 | 1723.13 |
| $S_1(11,9)$ | 2020 | 2035.96 | 2019.02 | 2019.83 | 2032.29 |

[a] The transitions are labeled "$S_v(J',J'')$."

[b] The experimental data were taken from CARS data given in refs 7 and 18.

Table 3. Computed energies of $H_2$ Q-branch transitions

| J | V = 0 | | V = 1 | |
|---|---|---|---|---|
| | Fink et al. | Ermler | Fink et al. | Ermler |
| 0 | 4161.18 | 4161.12 | 3925.82 | 3927.00 |
| 1 | 4155.25 | 4155.20 | 3919.99 | 3920.23 |
| 2 | 4143.32 | 4143.40 | 3908.16 | 3908.71 |
| 3 | 4125.21 | 4125.79 | 3890.00 | 3891.52 |
| 4 | 4100.68 | 4102.49 | 3865.00 | 3868.80 |
| 5 | 4069.40 | 4073.65 | 3832.52 | 3840.61 |
| 6 | 4030.94 | 4039.43 | 3791.70 | 3807.21 |
| 7 | 3984.82 | 4000.08 | 3741.56 | 3768.80 |
| 8 | 3930.44 | 3955.85 | 3680.93 | 3725.63 |
| 9 | 3867.15 | 3907.04 | 3608.47 | 3677.99 |
| 10 | 3794.19 | 3853.97 | 3522.70 | 3626.20 |
| 11 | 3710.74 | 3797.03 | 3421.95 | 3570.64 |
| 12 | 3615.89 | 3736.61 | 3304.38 | 3511.69 |
| 13 | 3508.63 | 3673.17 | 3168.01 | 3449.80 |
| 14 | 3387.88 | 3607.17 | 3010.67 | 3385.44 |
| 15 | 3252.49 | 3539.16 | 2830.03 | 3319.12 |
| 16 | 3101.21 | 3469.66 | 2623.60 | 3251.37 |
| 17 | 2932.70 | 3399.29 | 2388.70 | 3182.80 |
| 18 | 2745.56 | 3328.67 | 2122.53 | 3113.99 |
| 19 | 2538.28 | 3258.47 | 1822.07 | 3045.63 |
| 20 | 2309.30 | 3189.39 | 1484.18 | 2978.39 |

Table 4. Computed energies of $H_2$ S-branch transitions

| J' | J'' | V = 0 | | V = 1 | |
|---|---|---|---|---|---|
| | | Fink et al. | Ermler | Fink et al. | Ermler |
| 0 | 0 | 354.37 | 354.13 | 336.69 | 336.41 |
| 3 | 1 | 587.02 | 586.74 | 557.68 | 557.33 |
| 4 | 2 | 814.40 | 814.22 | 773.55 | 773.30 |
| 5 | 3 | 1034.65 | 1034.67 | 982.47 | 982.50 |
| 6 | 4 | 1246.16 | 1246.37 | 1182.79 | 1183.26 |
| 7 | 5 | 1447.61 | 1447.80 | 1373.12 | 1374.15 |
| 8 | 6 | 1638.11 | 1637.69 | 1552.39 | 1553.96 |
| 9 | 7 | 1817.18 | 1815.08 | 1719.90 | 1721.81 |
| 10 | 8 | 1984.89 | 1979.37 | 1875.37 | 1877.15 |
| 11 | 9 | 2141.91 | 2130.32 | 2019.02 | 2019.83 |
| 12 | 10 | 2289.56 | 2268.18 | 2151.61 | 2150.14 |
| 13 | 11 | 2429.91 | 2393.64 | 2274.49 | 2268.85 |
| 14 | 12 | 2565.84 | 2507.95 | 2389.67 | 2377.27 |
| 15 | 13 | 2701.09 | 2612.97 | 2499.89 | 2477.29 |
| 16 | 14 | 2840.35 | 2711.12 | 2608.65 | 2571.43 |
| 17 | 15 | 2989.33 | 2805.54 | 2720.27 | 2662.86 |
| 18 | 16 | 3154.84 | 2900.08 | 2839.97 | 2755.49 |
| 19 | 17 | 3344.84 | 2999.35 | 2973.92 | 2853.99 |
| 20 | 18 | 3568.49 | 3108.80 | 3129.26 | 2963.83 |
| 21 | 19 | 3836.30 | 3234.71 | 3314.22 | 3091.35 |

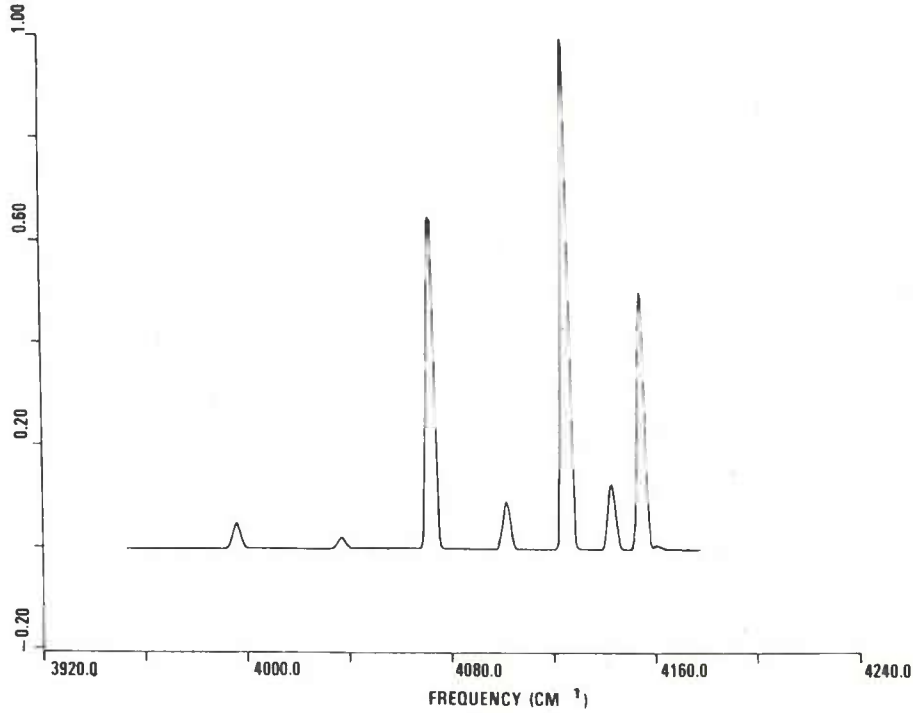


Figure 1. $H_2$ CARS Q-branch spectra at 2500 K

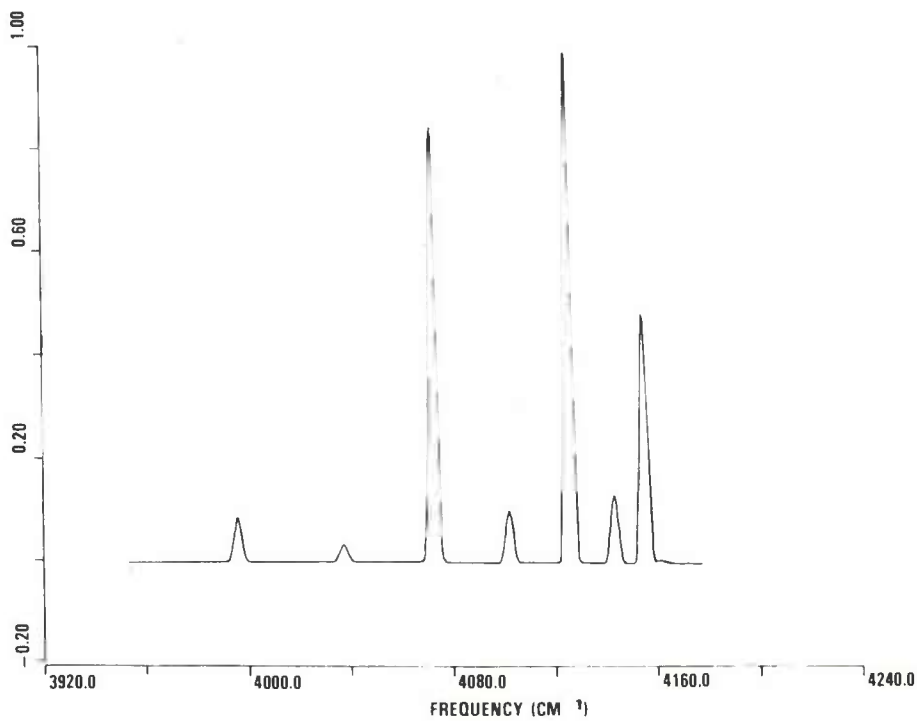


Figure 2. $H_2$ CARS Q-branch spectra at 3000 K

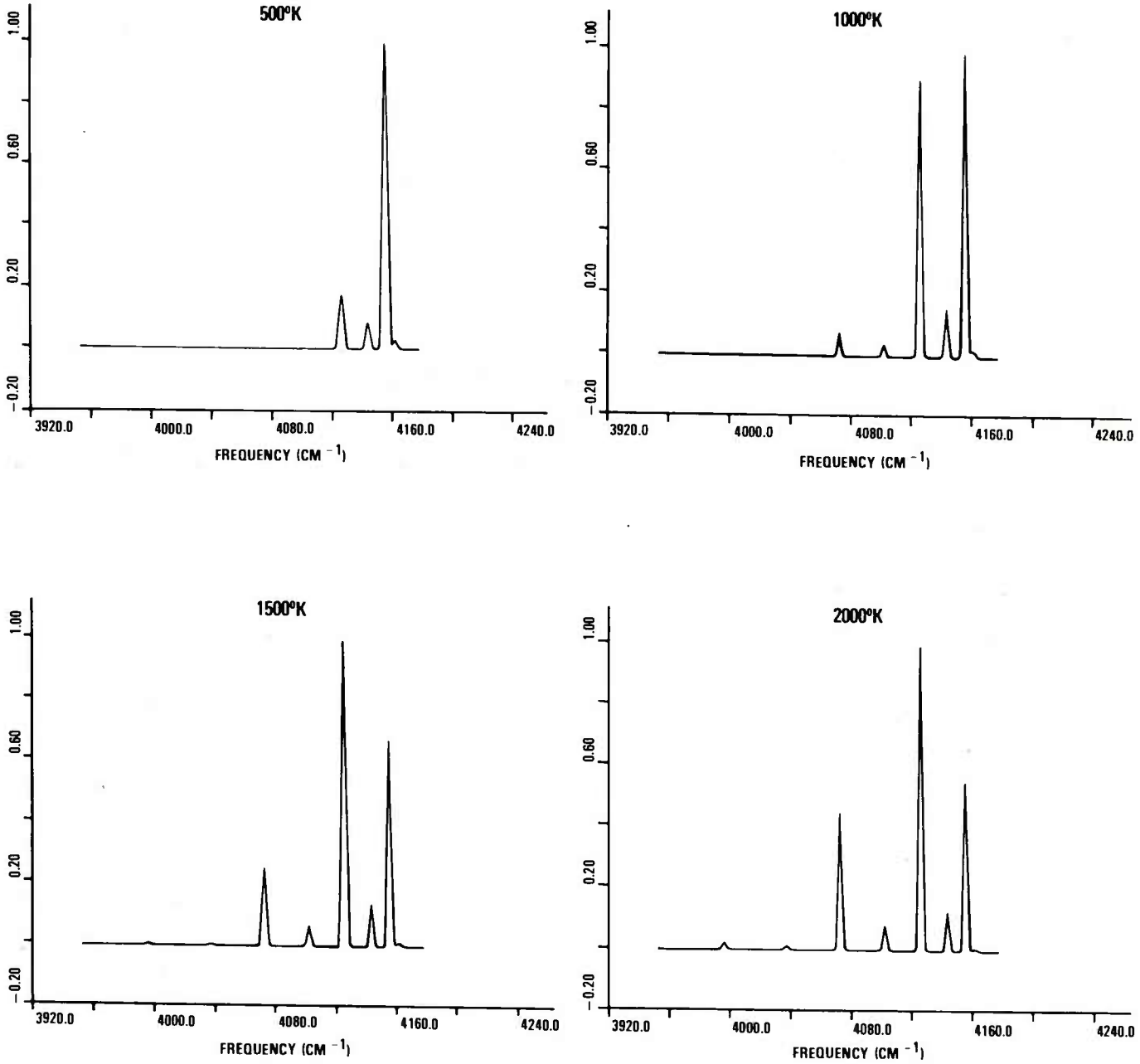


Figure 3. Temperature variation of $H_2$ CARS spectra

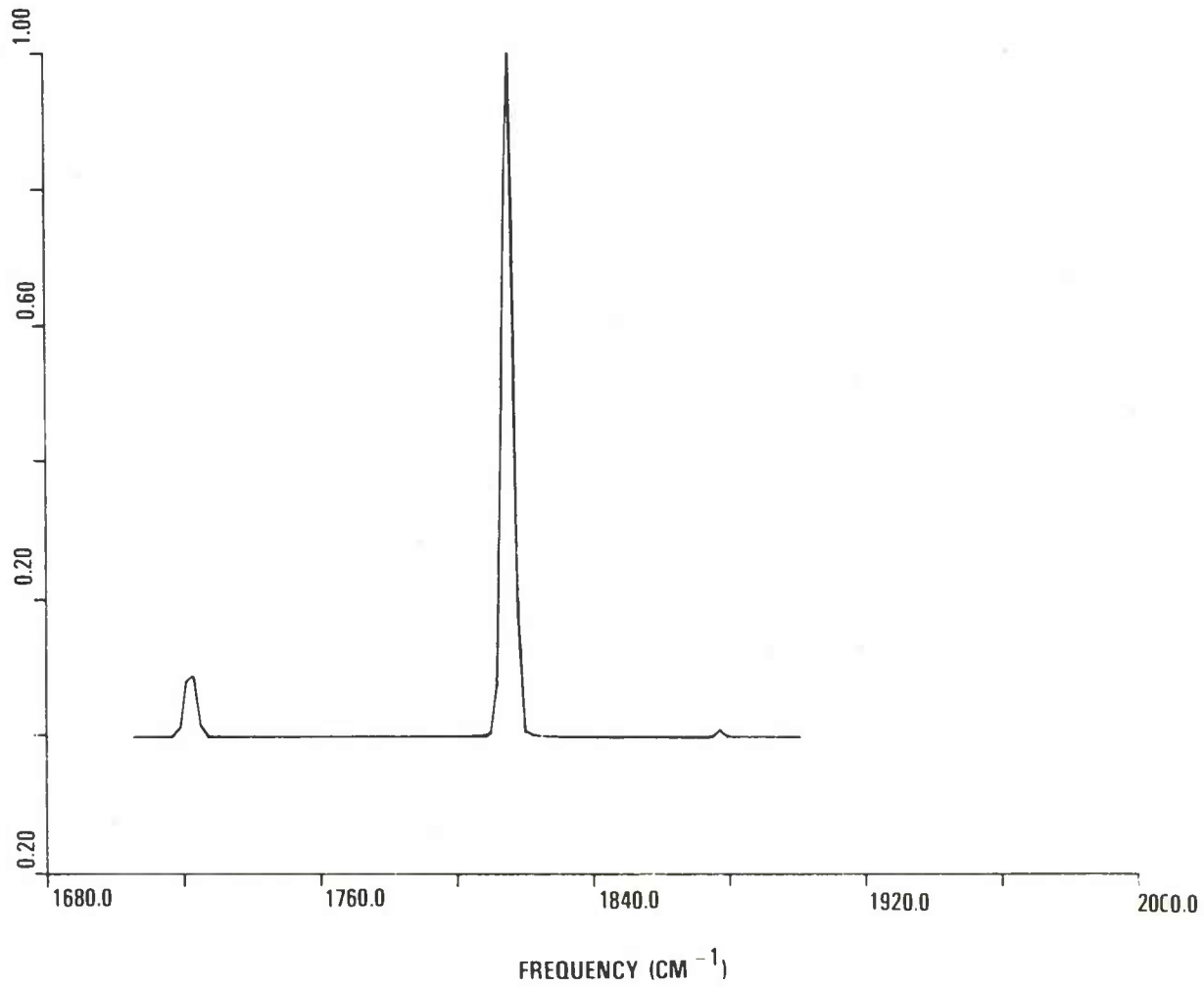


Figure 4. $H_2$ CARS S-branch at 2732 K

DISTRIBUTION LIST

Commander
Armament Research and Development Center
U.S. Army Armament, Munitions and
Chemical Command
ATTN: DRSMC-TSS(D) (5)
DRSMC-TDC(D), D. A. Gyorog
DRSMC-GCL(D)
DRSMC-LC(D), J. Frasier
J. P. Picard
DRSMC-LCA(D), T. Davidson
DRSMC-LCA-G(D), J. Lannon
D. Downs
L. Harris (10)
T. Vladimiroff
A. Beardell
Y. Carignon
J. Fendell (10)
K. Aron
E. Petrow
DRSMC-LCE(D), R. Walker
P. Marinkas
C. Capellos
F. Owens
S. Bulusu
F. Gilbert
Dover, NJ 07801

Administrator
Defense Technical Information Center
ATTN: Accessions Division (12)
Cameron Station
Alexandria, VA 22314

Director
U.S. Army Materiel Systems
Analysis Activity
ATTN: DRXSY-MP
Aberdeen Proving Ground, MD 21005

Commander
Chemical Research and Development Center
U.S. Army Armament, Munitions and
Chemical Command
ATTN: DRSMC-CLJ-L(A)
DRSMC-CLB-PA(A)
APG, Edgewood Area, MD 21010

Director
Ballistics Research Laboratory
Armament Research and Development Center
U.S. Army Armament, Munitions and
Chemical Command
ATTN: DRSMC-TSB-S(A)
DRSMC-BLP(A), L. Watermier
A. Barrows
G. Adams
R. Fifer
M. Miller
T. Coffee
J. Heimeryl
C. Nelson
J. Vanderhoff
J. Anderson
Aberdeen Proving Ground, MD 21005

Chief
Benet Weapons Laboratory, LCWSL
Armament Research and Development Center
U.S. Army Armament, Munitions and
Chemical Command
ATTN: DRSMC-LCB-TL
Watervliet, NY 12189

Commander
U.S. Army Armament, Munitions and
Chemical Command
ATTN: DRSMC-LEP-L(R)
Rock Island, IL 61299

Director
U.S. Army TRADOC Systems
Analysis Activity
ATTN: ATAA-SL
White Sands Missile Range, NM 88002

Director
Defense Advanced Research Projects
Agency
ATTN: LTC C. Buck
1400 Wilson Boulevard
Arlington, VA 22209

Commander
U.S. Army Materiel Development
and Readiness Command
ATTN: DRCDMD-ST
5001 Eisenhower Avenue
Alexandria, VA 22333

Commander
U.S. Army Watervliet Arsenal
ATTN: SARWV-RD, R. Thierry
Watervliet, NY 12189

Director
U.S. Army Air Mobility Research
and Development Laboratory
Ames Research Center
Moffett Field, CA 94035

Commander
U.S. Army Communications Research
and Development Command
ATTN: DRDCO-PPA-SA
Fort Monmouth, NJ 07703

Commander
U.S. Army Electronics Research
and Development Command
Technical Support Activity
ATTN: DELSD-L
Fort Monmouth, NJ 07703

Commander
U.S. Army Missile Command
ATTN: DRSMI-R
DRSMI-YDL
Redstone Arsenal, AL 35809

Commander
U.S. Army Natick Research
and Development Command
ATTN: DRXRE, D. Sieling
Natick, MA 01762

Commander
U.S. Army Tank Automotive Research
and Development Command
ATTN: DRDTA-UL
Warren, MI 48090

Commander
U.S. Army White Sands Missile Range
ATTN: STEWS-VT
White Sands Missile Range, NM 88002

Commander
U.S. Army Materials and
Mechanics Research Center
ATTN: DRXMR-ATL
Watertown, MA 02172

Commander
U.S. Army Research Office
ATTN: Technical Library
D. Squire
F. Schmiedeshaff
R. Ghirardelli
M. Ciftan
P.O. Box 12211
Research Triangle Park, NC 27706

Office of Naval Research
ATTN: Code 473
G. Neece
800 N. Quincy Street
Arlington, VA 22217

Commander
Naval Sea Systems Command
ATTN: J. W. Murrin, SEA-62R2
National Center
Bldg 2, Room 6E08
Washington, DC 20362

Commander
Naval Surface Weapons Center
ATTN: Library Branch, DX-21
Dahlgren, VA 22448

Commander
Naval Surface Weapons Center
ATTN: Code 240, S. J. Jacobs, J. Sharma
Code 730
Silver Spring, MD 20910

Commander
Naval Underwater Systems Center
Energy Conversion Department
ATTN: Code 5B331, R. S. Lazar
Newport, RI 02840

Commander
Naval Weapons Center
ATTN: R. Derr
C. Thelen
China Lake, CA 93555

Commander
Naval Research Laboratory
ATTN: Code 6180
Washington, DC 20375

Superintendent
Naval Postgraduate School
ATTN: Technical Library
D. Netzer
A. Fuhs
Monterey, CA 93940

Commander
Naval Ordnance Station
ATTN: Dr. Charles Dale
Technical Library
Indian Head, MD 20640

AFOSR
ATTN: J. F. Masi
B. T. Wolfson
D. Ball
L. Caveny
Bolling AFB, DC 20332

AFRPL (DYSC)
ATTN: D. George
J. N. Levine
Edwards AFB, CA 93523

National Bureau of Standards
ATTN: J. Hastie
T. Kashiwagi
H. Semerjian
M. Jacox
K. Smyth
J. Stevenson
Washington, DC 20234

Lockheed Palo Alto Research Laboratories
ATTN: Technical Information Center
3521 Hanover Street
Palo Alto, CA 94304

Aerojet Solid Propulsion Co.
ATTN: P. Micheli
Sacramento, CA 95813

ARO Incorporated
ATTN: N. Dougherty
Arnold AFS, TN 37389

Atlantic Research Corporation
ATTN: M. K. King
5390 Cherokee Avenue
Alexandria, VA 22314

AVCO Corporation
AVCO Everett Research Laboratory
Division
ATTN: D. Stickler
2385 Revere Beach Parkway
Everett, MA 02149

Calspan Corporation
ATTN: E. B. Fisher
A. P. Trippe
P.O. Box 400
Buffalo, NY 14221

Foster Miller Associates, Inc.
ATTN: A. J. Erickson
135 Second Avenue
Waltham, MA 02154

General Electric Company
Armament Department
ATTN: M. J. Bulman
Lakeside Avenue
Burlington, VT 05402

General Electric Company
Flight Propulsion Division
ATTN: Technical Library
Cincinnati, OH 45215

Hercules Incorporated
Alleghany Ballistic Lab
ATTN: R. Miller
Technical Library
Cumberland, MD 21501

Hercules Incorporated
Bacchus Works
ATTN: B. Isom
Magna, UT 84044

IITRI
ATTN: M. J. Klein
10 West 35th Street
Chicago, IL 60615

Olin Corporation
Badger Army Ammunition Plant
ATTN: J. Ramnarace
Baraboo, WI 53913

Olin Corporation
New Haven Plant
ATTN: R. L. Cook
D. W. Riefler
275 Winchester Avenue
New Haven, CT 06504

Paul Gough Associates, Inc.
ATTN: P. S. Gough
P.O. Box 1614
Portsmouth, NH 03801

Physics International Company
2700 Merced Street
Leandro, CA 94577

Pulsepower Systems, Inc.
ATTN: L. C. Elmore
815 American Street
San Carlos, CA 94070

Rockwell International Corp.
Rocketdyne Division
ATTN: C. Obert
J. E. Flanagan
A. Axeworthy
6633 Canoga Avenue
Canoga Park, CA 91304

Rockwell International Corp.
Rocketdyne Division
ATTN: W. Haymes
Technical Library
McGregor, TX 76657

Science Applications, Inc.
ATTN: R. B. Edelman
Combustion Dynamics and
Propulsion Division
23146 Cumorah Crest
Woodland Hills, CA 91364

Shock Hydrodynamics, Inc.
ATTN: W. H. Anderson
4710-16 Vineland Avenue
N. Hollywood, CA 91602

Thiokol Corporation
Elkton Division
ATTN: E. Sutton
Elkton, MD 21921

Thiokol Corporation
Huntsville Division
ATTN: D. Flanigan
R. Glick
Technical Library
Huntsville, AL 35807

Thiokol Corporation
Wasatch Division
ATTN: J. Peterson
Technical Library
P.O. Box 524
Brigham City, UT 84302

TRW Systems Group
ATTN: H. Korman
One Space Park
Redondo Beach, CA 90278

United Technologies
Chemical Systems Division
ATTN: R. Brown
Technical Library
P.O. Box 358
Sunnyvale, CA 94086

Battelle Memorial Institute
ATTN: Technical Library
R. Bartlett
505 King Avenue
Columbus, OH 43201

Brigham Young University
Department of Chemical Engineering
ATTN: M. W. Beckstead
Provo, UT 84601

California Institute of Technology
204 Karmar Lab
Mail Stop 301-46
ATTN: F. E. C. Culick
1201 E. California Street
Pasadena, CA 91125

Case Western Reserve University
Division of Aerospace Sciences
ATTN: J. Tien
Cleveland, OH 44135

Georgia Institute of Technology
School of Aerospace Engineering
ATTN: B. T. Zinn
E. Price
W. C. Strahle
Atlanta, GA 30332

Institute of Gas Technology
ATTN: D. Gidaspow
3424 S. State Street
Chicago, IL 60616

Johns Hopkins University/APL
Chemical Propulsion Information Agency
ATTN: T. Christian
Johns Hopkins Road
Laurel, MD 20810

Massachusetts Institute of Technology
Department of Mechanical Engineering
ATTN: T. Toong
Cambridge, MA 02139

Pennsylvania State University
Applied Research Laboratory
ATTN: G. M. Faeth
P.O. Box 30
State College, PA 16801

Pennsylvania State University
Department of Mechanical Engineering
ATTN: K. Kuo
University Park, PA 16801

Pennsylvania State University
Department of Material Sciences
ATTN: H. Palmer
University Park, PA 16801

Princeton Combustion Research
Laboratories
ATTN: M. Summerfield
N. Messina
1041 U.S. Highway One North
Princeton, NJ 08540

Princeton University
Forrestal Campus
ATTN: I. Glassman
F. Dryer
Technical Library
P.O. Box 710
Princeton, NJ 08540

Purdue University
School of Mechanical Engineering
ATTN: J. Osborn
S. N. B. Murthy
N. M. Laurendeau
TSPC Chaffee Hall
W. Lafayette, IN 47906

Rutgers State University
Department of Mechanical and
Aerospace Engineering
ATTN: S. Temkin
University Heights Campus
New Brunswick, NJ 08903

SRI International
ATTN: Technical Library
D. Crosley
J. Barker
D. Golden
333 Ravenswood Avenue
Menlo Park, CA 94025

Stevens Institute of Technology
W. C. Ermler
Department of Chemistry and Chemical Engineering
Hoboken, NJ 07030

United Technology
ATTN: Alan Ecbreth
Robert Hall
Research Center
East Hartford, CT 06108

Commander
Naval Research Laboratory
Chemistry Division
ATTN: A. Harvey
Washington, DC 20375

General Motors Research Laboratory
ATTN: J. H. Bechtel
Warren, Michigan 48090

System Research Laboratory
ATTN: L. Goss
2600 Indian Ripple Rd
Dayton, Ohio 45440

Exxon Research and Engineering
ATTN: A. Dean
M. Chou
P.O. Box 45
Linden, NJ 07036

Ford Motor Company
Research Staff
ATTN: K. Marko
L. Rimai
Dearborn, Michigan 48120

Sandia Laboratories
Applied Physics Division I
ATTN: L. Rahn
D. Stephenson
Livermore, CA 94550

Rensselaer Polytechnic Institute
Dept. of Chem. Engineering
ATTN: A. Fontijn
Troy, NY 12181

University of California,
San Diego
Ames Department
ATTN: F. Williams
P.O. Box 109
La Jolla, CA 92037

University of California
Dept. of Mechanical Eng.
ATTN: J. W. Daily
Berkeley, CA 94720

University of Dayton
University of Dayton Research Inst.
Dayton, OH 45406

University of Florida
Dept. of Chemistry
ATTN: J. Winefordner
Gainesville, Florida 32601

University of Illinois
Dept. of Mechanical Eng.
ATTN: H. Krier
144 MEB, 1206 W. Green St.
Urbana, IL 61801

University of Minnesota
Dept. of Mechanical Eng.
ATTN: E. Fletcher
Minneapolis, MN 55455

University of California,
Santa Barbara
Quantum Institute
ATTN: K. Schofield
M. Steinberg
Santa Barbara, CA 93106

University of Southern California
Department of Chemistry
ATTN: S. Benson
Los Angeles, CA 90007

Stanford University
Department of Mech. Eng.
ATTN: R. Hanson
Stanford, CA 93106

University of Texas
Department of Chemistry
ATTN: W. Gardiner
H. Schaefer
Austin, TX 78712

University of Utah
Dept. of Chemical Engineering
ATTN: A. Baer
G. Flandro
Salt Lake City, UT 84112